Precollisional velocity correlations in a hard-disk fluid with dissipative collisions

R. Soto,[1,2] J. Piasecki,[3] and M. Mareschal[1]
[1]*CECAM, ENS-Lyon, 46 Allée d'Italie, 69007 Lyon, France*
[2]*Departamento de Física, FCFM, Universidad de Chile, Casilla 487-3, Santiago, Chile*
[3]*Institute of Theoretical Phyiscs, University of Warsaw, Hoża 69, 00 681 Warsaw, Poland*
(Received 19 March 2001; published 29 August 2001)

Velocity correlations are studied in granular fluids, modeled by the inelastic hard sphere gas. Making a density expansion of the Bogoliubov-Born-Green-Kirkwood-Yvon hierarchy for the evolution of the reduced distributions, we predict the presence of precollisional velocity correlations. They are created by the propagation through correlated sequences of collisions (ring events) of the velocity correlations generated after dissipative collisions. The correlations have their origin in the dissipative character of collisions, being always present in granular fluids. The correlations, that manifest microscopically as an alignment of the velocities of a colliding pair produce modifications of collisional averages, in particular, the virial pressure. The pressure shows a reduction with respect to the elastic case as a consequence of the velocity alignment. Good qualitative agreement is obtained for the comparison of the numerical evaluations of the obtained analytical expressions and molecular dynamics results that showed evidence of precollisional velocity correlations [R. Soto and M. Mareschal, Phys. Rev. E **63**, 041303 (2001)].

DOI: 10.1103/PhysRevE.64.031306 PACS number(s): 45.70.Mg, 05.20.Dd

I. INTRODUCTION

Granular matter is characterized by energy dissipation at collisions. If energy is continuously injected into granular systems, they become fluidized. Granular fluids resemble elastic fluids, and kinetic and hydrodynamic descriptions have been used in their description. In the theory of granular fluids, the simplest model describing the effects of inelasticity is the inelastic hard sphere (IHS) fluid. Grains are represented by impenetrable hard spheres of diameter σ and mass m. The motion of the spheres between collisions is free. At a binary encounter the velocities $\mathbf{v}_1$, $\mathbf{v}_2$ of the colliding pair suffer the instantaneous transformation

$$\mathbf{v}_1 \to \mathbf{v}_1' = \mathbf{v}_1 - \frac{1}{2}(1+\alpha)(\hat{\sigma}\cdot\mathbf{v}_{12})\hat{\sigma}, \tag{1}$$

$$\mathbf{v}_2 \to \mathbf{v}_2' = \mathbf{v}_2 + \frac{1}{2}(1+\alpha)(\hat{\sigma}\cdot\mathbf{v}_{12})\hat{\sigma}.$$

Here $\hat{\sigma}$ is the unit vector oriented along the line passing through the centers of the spheres at the moment of the impact, $\mathbf{v}_{12}=\mathbf{v}_1-\mathbf{v}_2$, and $0\leqslant\alpha\leqslant 1$ is the restitution coefficient, measuring the degree of inelasticity. The transformation (1) conserves momentum but, when $\alpha<1$, does not conserve energy. The loss of energy equals

$$\frac{1}{2}m(v_1'^2+v_2'^2-v_1^2-v_2^2) = -\frac{m}{4}(1-\alpha^2)(\hat{\sigma}\cdot\mathbf{v}_{12})^2. \tag{2}$$

When $\alpha=1$, energy conserving elastic collisions are recovered. It is useful to define the inelasticity coefficient $q=(1-\alpha)/2$, that vanishes in the elastic limit.

The precollision velocities $(\mathbf{v}_1^*, \mathbf{v}_2^*)$ leading to the velocities $(\mathbf{v}_1, \mathbf{v}_2)$ are found by inverting the collision law (1),

$$\mathbf{v}_1^* = \mathbf{v}_1 - \frac{1}{2}(1+\alpha^{-1})(\hat{\sigma}\cdot\mathbf{v}_{12})\hat{\sigma}, \tag{3}$$

$$\mathbf{v}_2^* = \mathbf{v}_2 + \frac{1}{2}(1+\alpha^{-1})(\hat{\sigma}\cdot\mathbf{v}_{12})\hat{\sigma}.$$

The present paper is concerned with dynamic correlations in fluidized granular matter, represented by the two-dimensional IHS model. Our object is to study precollisional correlations at the microscopic length scale, of the order of the hard sphere diameter. This question has not yet been sufficiently discussed. First studies of correlations, based on fluctuating hydrodynamics and on the ring kinetic equation, were focused on the effects of inelasticity on the large distance structure of the fluid [1–3]. At weak inelasticities algebraic r^{-d} tails have been found in the spatial velocity correlations, with an exponential cutoff at distances r of the order of the density instability length scale.

At short length scales, the mechanism of creation of postcollisional velocity correlations has been studied in detail. It turns out that the hard sphere dynamics implies a relation between the two-particle density of precollisional and postcollisional states [4]. In the IHS model it takes the form

$$\Theta(-\mathbf{r}_{12}\cdot\mathbf{v}_{12})\frac{1}{\alpha^2}f_2(\mathbf{r}_1,\mathbf{v}_1,\mathbf{r}_1-\sigma\hat{\sigma},\mathbf{v}_2,t) = \Theta(\mathbf{r}_{12}\cdot\mathbf{v}_{12}')f_2(\mathbf{r}_1,\mathbf{v}_1',\mathbf{r}_1-\sigma\hat{\sigma},\mathbf{v}_2',t), \tag{4}$$

where Θ is the unit step function and f_2 denotes the two-particle reduced density. Equation (4) implies that for $\alpha<1$, f_2 is discontinuous at contact ($|\mathbf{r}_{12}|=\sigma$) when passing from the hemisphere $\mathbf{r}_{12}\cdot\mathbf{v}_{12}<0$ (precollisional configuration) to the hemisphere $\mathbf{r}_{12}\cdot\mathbf{v}_{12}>0$ (postcollisional configu-

ration) [5]. It also follows from Eq. (4) that uncorrelated precollisional states become correlated after a binary collision.

In Ref. [5] the presence of precollisional velocity correlations has also been observed with the use of molecular dynamics simulations. It is the aim of the present paper to study the precollisional correlations in a systematic way starting from the microscopic equations of motion. This issue is of primary importance for the applicability to granular fluids of the Boltzmann and of the Enskog kinetic theories, as both of them neglect these correlations. It should be stressed that in contradistinction to elastic fluids, the IHS model has no equilibrium state with uncorrelated velocities.

Our study is of fundamental nature. Therefore, we chose an idealized initial condition and the low density limit in order to study in a transparent way the effect of dissipative collisions in the generation of precollisional velocity correlations.

In Sec. II the hierarchy equations are used to derive the formulas for the lowest order in density and in inelasticity contributions to the precollisional velocity correlations. They result from the propagation of the postcollisional correlations through correlated sequences of binary collisions. In Sec. III the effect of correlations on some collisional averages is computed. In particular the modification they introduce into the virial pressure is discussed therein. In Sec. IV we compare the analytic results with molecular dynamics simulations. Section V contains concluding remarks.

II. PRECOLLISIONAL VELOCITY CORRELATIONS

In what follows, we will study two-dimensional (2D) systems. The extension to three dimensions is straightforward. We adopt the short-hand notation

$$j \equiv (\mathbf{r}_j, \mathbf{v}_j), \quad j = 1,2,\ldots, \tag{5}$$

for one-particle states, where $\mathbf{r}_j$, $\mathbf{v}_j$ are the position and the velocity vectors, respectively.

At time t, the state of the fluid can be described by the set of reduced distributions $f_s(1,2,\ldots,s;t)$, $s=1,2,\ldots$, representing the densities of s-particle configurations.

The evolution of the state of the fluid in the course of time can be conveniently described with the use of the binary collision operator $\overline{T}^{\alpha}(i,j)$, corresponding to the inverse collision law (3). In two-dimensions $\overline{T}^{\alpha}(i,j)$ acts on a function $\Psi(\mathbf{r}_i,\mathbf{v}_i,\mathbf{r}_j,\mathbf{v}_j)$ according to the formula [6,2]

$$\begin{aligned}\overline{T}^{\alpha}&\Psi(\mathbf{r}_i,\mathbf{v}_i,\mathbf{r}_j,\mathbf{v}_j)\\ &= \sigma \int d\hat{\sigma}(\hat{\sigma}\cdot\mathbf{v}_{ij})\Theta(\hat{\sigma}\cdot\mathbf{v}_{ij})\left\{\frac{1}{\alpha^2}\delta(\mathbf{r}_{ij}-\sigma\hat{\sigma})b^{*}_{\hat{\sigma}}(ij)\right.\\ &\left. - \delta(\mathbf{r}_{ij}+\sigma\hat{\sigma})\right\}\Psi(\mathbf{r}_i,\mathbf{v}_i,\mathbf{r}_j,\mathbf{v}_j),\end{aligned} \tag{6}$$

where

$$b^{*}_{\hat{\sigma}}(ij)\Psi(\mathbf{r}_i,\mathbf{v}_i,\mathbf{r}_j,\mathbf{v}_j) = \Psi(\mathbf{r}_i,\mathbf{v}_i^{*},\mathbf{r}_j,\mathbf{v}_j^{*}), \tag{7}$$

where Θ denotes the unit step function and δ is the Dirac distribution.

In order to write down the Bogoliubov-Born-Green-Kirkwood-Yvon (BBGKY) hierarchy coupling the evolution of the distributions $f_s(1,\ldots,s;t)$, we introduce the generator of the s-particle free streaming

$$\mathcal{L}_0(1,\ldots,s) = \sum_{j=1}^{s}\mathcal{L}_0(j) = \sum_{j=1}^{s}\mathbf{v}_j\cdot\frac{\partial}{\partial\mathbf{r}_j} \tag{8}$$

and the generator of the full s-particle dynamics

$$\mathcal{L}^{\alpha}(1,\ldots,s) = \mathcal{L}_0(1,\ldots,s) - \sum_{i<j}^{s}\overline{T}^{\alpha}(ij). \tag{9}$$

The BBGKY hierarchy reads [6,2]

$$\left\{\frac{\partial}{\partial t}+\mathcal{L}_0(1)\right\}f_1(1;t) = \int d2\,\overline{T}^{\alpha}(12)f_2(12;t), \tag{10}$$

$$\begin{aligned}&\left\{\frac{\partial}{\partial t}+\mathcal{L}^{\alpha}(1,\ldots,s)\right\}f_s(1,\ldots,s;t)\\ &\quad = \sum_{j=1}^{s}\int d(s+1)\overline{T}^{\alpha}(j,s+1)f_{s+1}(1,\ldots,s,s+1;t),\end{aligned}$$

$$s = 2,3,\ldots. \tag{11}$$

The notation $dj = d\mathbf{r}_j d\mathbf{v}_j$ has been used in writing Eqs. (10) and (11).

Suppose that at the initial moment $t=0$ the fluid is in thermal equilibrium at some temperature T. The reduced distributions have the form

$$f_s(1,\ldots,s;0) = n^s g_s^{\mathrm{eq}}(\mathbf{r}_1,\ldots,\mathbf{r}_s)\prod_{j=1}^{s}\varphi_T(v_j), \tag{12}$$

where n is the number density of the particles, g_s^{eq} is the configurational s-particle distribution, and

$$\varphi_T(v) = \frac{m}{2\pi T}\exp\left\{-\frac{mv^2}{2T}\right\} \tag{13}$$

is the Maxwell distribution in 2D.

The equilibrium state (12) is invariant under the elastic hard disk dynamics with $\alpha=1$. However, when $\alpha<1$, dissipation of energy occurs [see Eq. (2)], and inelastic collisions (1) imply the process of cooling down. Although the initial state (12) does not contain any correlations between the velocities, the dissipative dynamics, contrary to the elastic one, does create them. It is why the choice of the initial state (12) permits to study purely dissipative effects.

Our object here is to study the precollisional correlations resulting from the inelastic character of collisions. We shall thus be interested in determining the structure of the two-particle density $f_2(12;t)$ in the precollisional phase-space region

$$\mathbf{r}_{12}\cdot\mathbf{v}_{12}<0,$$
$$|\mathbf{r}_{12}|=\sigma^{+}. \tag{14}$$

To this end we shall use the formal solution of the hierarchy (10), expressed in terms of the initial condition. The general equation (11) can be rewritten as

$$f_s(1,\ldots,s;t)=e^{-t\mathcal{L}^{\alpha}(1,\ldots,s)}f_s(1,\ldots,s;0)+\sum_{j=1}^{s}\int_0^t d\tau\, e^{-(t-\tau)\mathcal{L}^{\alpha}(1,\ldots,s)}\int d(s+1)\times\overline{T}^{\alpha}(j,s+1)f_{s+1}(1,\ldots,s,s+1;\tau). \tag{15}$$

Using Eq. (15) and keeping only two- and three-body propagators in the expression for $f_2(12;t)$, which corresponds to the lowest order terms in the density expansion of the dynamics, we find

$$\frac{1}{n^2}f_2(12;t)=e^{-t\mathcal{L}^{\alpha}(12)}g_2^{\mathrm{eq}}(\mathbf{r}_{12})\varphi_T(v_1)\varphi_T(v_2)+n\int_0^t d\tau\int d3\times e^{-(t-\tau)[\mathcal{L}^{\alpha}(12)+\mathcal{L}_0(3)]}[\overline{T}^{\alpha}(13)+\overline{T}^{\alpha}(23)]e^{-\tau\mathcal{L}^{\alpha}(123)}\times g_3^{\mathrm{eq}}(\mathbf{r}_1,\mathbf{r}_2,\mathbf{r}_3)\varphi_T(v_1)\varphi_T(v_2)\varphi_T(v_3)+\cdots. \tag{16}$$

The initial condition (12) has been used in writing Eq. (16). The formula (16) for f_2 is physically valid at the short time scale of the order of few mean free times because, starting from the initial moment, only the dynamics of two and three isolated groups of particles is taken into account.

In what follows we will retain only those terms in Eq. (16) that contribute to velocity correlations in the precollisional region (14). The first term on the right-hand side of Eq. (16) involves two-particle dynamics with no precollisional correlations. The second term can be conveniently rewritten in the form

$$n\int d3\,\{e^{-t\mathcal{L}^{\alpha}(123)}-e^{-t[\mathcal{L}^{\alpha}(12)+\mathcal{L}_0(3)]}\}\times g_3^{\mathrm{eq}}(\mathbf{r}_1,\mathbf{r}_2,\mathbf{r}_3)\prod_{j=1}^{3}\varphi_T(v_j). \tag{17}$$

To the lowest order in density

$$g_3^{\mathrm{eq}}(\mathbf{r}_1,\mathbf{r}_2,\mathbf{r}_3)=\prod_{j=1}^{3}\Theta(|\mathbf{r}_{ij}|-\sigma). \tag{18}$$

We define

$$f^{\mathrm{eq}}(123)\equiv\prod_{j=1}^{3}\Theta(|\mathbf{r}_{ij}|-\sigma)\prod_{j=1}^{3}\varphi_T(v_j). \tag{19}$$

The precollisional velocity correlations are created by three-particle processes contributing to the term

$$n\int d3\,e^{-t\mathcal{L}^{\alpha}(123)}f^{\mathrm{eq}}(123) \tag{20}$$

in Eq. (17). Using the relation

$$\mathcal{L}(123)f^{\mathrm{eq}}(123)=0, \tag{21}$$

where $\mathcal{L}(123)=\mathcal{L}^{\alpha=1}(123)$ is the generator of the elastic three-particle dynamics, we find

$$\begin{aligned}n\int d3\,e^{-t\mathcal{L}^{\alpha}(123)}f^{\mathrm{eq}}(123)&=n\int d3\left\{e^{-t\mathcal{L}(123)}+\int_0^t d\tau\frac{\partial}{\partial\tau}\times[e^{-\tau\mathcal{L}^{\alpha}(123)}e^{-(t-\tau)\mathcal{L}(123)}]\right\}f^{\mathrm{eq}}(123)\\&=n\int d3\left\{f^{\mathrm{eq}}(123)+\int_0^t d\tau\, e^{-\tau\mathcal{L}^{\alpha}(123)}\times\sum_{i<j}^{3}[\overline{T}^{\alpha}(ij)-\overline{T}(ij)]f^{\mathrm{eq}}(123)\right\}.\end{aligned} \tag{22}$$

Only the last term in Eq. (22) contains the velocity correlations. We focus here our attention on its form close to the elastic limit $\alpha\to1$. Using the definitions (6) and (7) we get

$$[\overline{T}^{\alpha}(ij)-\overline{T}(ij)]f^{\mathrm{eq}}(123)=f^{\mathrm{eq}}(123)\sigma\int d\hat{\sigma}(\hat{\sigma}\cdot\mathbf{v}_{ij})\Theta(\hat{\sigma}\cdot\mathbf{v}_{ij})\times\delta(\mathbf{r}_{ij}-\sigma\hat{\sigma})H^{\alpha}(\hat{\sigma}\cdot\mathbf{v}_{ij}), \tag{23}$$

where

$$\begin{aligned}H^{\alpha}(\hat{\sigma}\cdot\mathbf{v}_{ij})&=\frac{1}{\alpha^2}\exp\left\{-\frac{m(1-\alpha^2)}{4T\alpha^2}(\hat{\sigma}\cdot\mathbf{v}_{ij})^2\right\},\\&=qh(\hat{\sigma}\cdot\mathbf{v}_{ij})+\mathcal{O}(q^2),\end{aligned} \tag{24}$$

with

$$h(\hat{\sigma}\cdot\mathbf{v}_{ij})=4\left[1-\frac{m}{4T}(\hat{\sigma}\cdot\mathbf{v}_{ij})^2\right]. \tag{25}$$

Inserting Eqs. (23) and (24) into Eq. (22) and keeping only the term linear in q we arrive at the following representation of the term responsible for precollisional correlations

$$qn\int d3\,f^{\mathrm{eq}}(123)\int_0^t d\tau\, e^{-\tau\mathcal{L}(123)}\sum_{i<j}^{3}\sigma\int d\hat{\sigma}(\hat{\sigma}\cdot\mathbf{v}_{ij})\times\Theta(\hat{\sigma}\cdot\mathbf{v}_{ij})\,\delta(\mathbf{r}_{ij}-\sigma\hat{\sigma})h(\hat{\sigma}\cdot\mathbf{v}_{ij}). \tag{26}$$

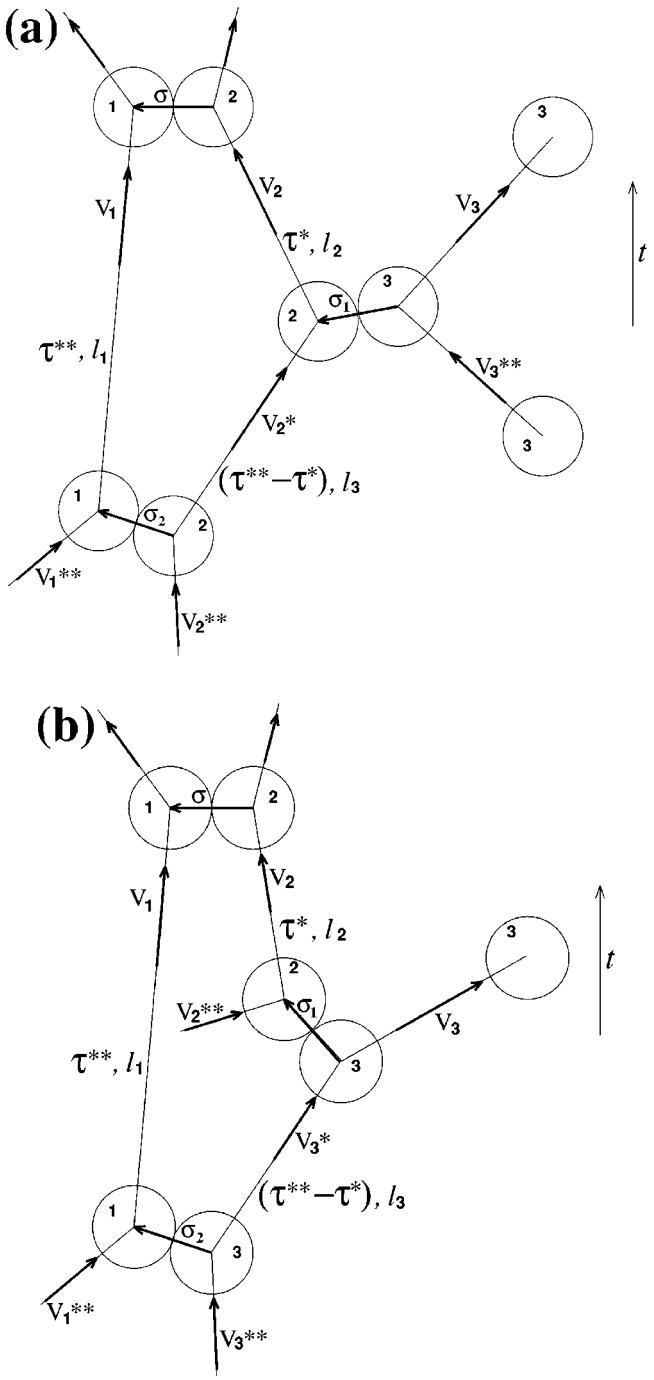

FIG. 1. Dynamical event corresponding to (a) $I_t(23,12)$ and (b) $I_t(23,13)$. The dynamical events corresponding to $I_t(13,12)$ and $I_t(13,23)$ are obtained replacing the role of particles 1 and 2 in (a) and (b), respectively. The duration of the internal free flights are τ, τ^*, and $(\tau^{**}-\tau^*)$; and the distance traveled in the flights are l_1, l_2, and l_3.

It is known that the three-particle elastic hard disk propagator $\exp[-\tau\mathcal{L}(123)]$ has a finite binary collision expansion, because between three hard disks on an infinite plane at most four collisions can occur [7]. We shall study here dynamical events involving sequences of three collisional configurations. The case of four collisions occurs rarely, and will not be considered.

Inserting into Eq. (26) the binary collision expansion

$$e^{-\tau_1\mathcal{L}(123)}=e^{-\tau_1\mathcal{L}_0(123)}+\int_0^{\tau_1}d\tau_2\,e^{-(\tau_1-\tau_2)\mathcal{L}_0(123)}\times[\mathcal{L}_0(123)-\mathcal{L}(123)]e^{-\tau_2\mathcal{L}_0(123)}+\cdots, \tag{27}$$

we find the sum of four terms corresponding to the so-called ring events. The graphical representation is given in Fig. 1. Analytically, we have to evaluate the expression

$$\Theta(-\mathbf{r}_{12}\cdot\mathbf{v}_{12})qn\int d3\{I_t(23,12)+I_t(13,12)+I_t(23,13)+I_t(13,23)\}\big|_{|\mathbf{r}_{12}|=\sigma^+}, \tag{28}$$

where

$$I_t(ab,ij)=f^{\mathrm{eq}}(123)\int_0^t d\tau_1\int_0^{\tau_1}d\tau_2\,e^{-(\tau_1-\tau_2)\mathcal{L}_0(123)}\sigma\times\int d\hat{\sigma}_1(\hat{\sigma}_1\cdot\mathbf{v}_{ab})\Theta(\hat{\sigma}_1\cdot\mathbf{v}_{ab})\delta(\mathbf{r}_{ab}-\sigma\hat{\sigma}_1)\times b^*_{\hat{\sigma}_1}(ab)e^{-\tau_2\mathcal{L}_0(123)}\sigma\int d\hat{\sigma}_2(\hat{\sigma}_2\cdot\mathbf{v}_{ij})\times\Theta(\hat{\sigma}_2\cdot\mathbf{v}_{ij})\delta(\mathbf{r}_{ij}-\sigma\hat{\sigma}_2)h(\hat{\sigma}_2\cdot\mathbf{v}_{ij}). \tag{29}$$

The time integrations in Eq. (29) can be performed owing to the presence of two delta distributions. After rather lengthy but straightforward calculations one finds

$$I_t(23,12)=f^{\mathrm{eq}}(123)\Theta(\mathbf{r}_{23}\cdot\mathbf{v}_{23})\Theta[\sigma^2-|\mathbf{r}_{23}|^2+(\mathbf{r}_{23}\cdot\mathbf{v}_{23})^2]\times\Theta[(\mathbf{v}_1-\mathbf{v}_2^*)\cdot(\mathbf{r}_{12}-\mathbf{v}_{12}\tau^*)]\times\Theta\left(\sigma^2-[\mathbf{r}_{12}-\mathbf{v}_{12}\tau^*]^2+\frac{1}{|\mathbf{v}_1-\mathbf{v}_2^*|^2}\times[(\mathbf{v}_1-\mathbf{v}_2^*)\cdot(\mathbf{r}_{12}-\mathbf{v}_{12}\tau^*)]^2\right)\Theta(\tau^{**}-\tau^*)\times\Theta(t-\tau^{**})h[\hat{\sigma}_2\cdot(\mathbf{v}_1-\mathbf{v}_2^*)], \tag{30}$$

with

$$|\mathbf{v}_{23}|\,\tau^*=\mathbf{r}_{23}\cdot\mathbf{v}_{23}/|\mathbf{v}_{23}|-\sqrt{\sigma^2-|\mathbf{r}_{23}|^2+(\mathbf{r}_{23}\cdot\mathbf{v}_{23}/|\mathbf{v}_{23}|)^2}, \tag{31}$$

$$\sigma\hat{\sigma}_1=\mathbf{r}_{23}-\mathbf{v}_{23}\tau^*,$$

$$\mathbf{v}_2^*=\mathbf{v}_2-(\mathbf{v}_{23}\cdot\hat{\sigma}_1)\hat{\sigma}_1,$$

$$|\mathbf{v}_1-\mathbf{v}_2^*|^2(\tau^{**}-\tau^*)=(\mathbf{r}_{12}-\mathbf{v}_{12}\tau^*)\cdot(\mathbf{v}_1-\mathbf{v}_2^*)-\sqrt{|\mathbf{v}_1-\mathbf{v}_2^*|^2[\sigma^2-(\mathbf{r}_{12}-\mathbf{v}_{12}\tau^*)^2]+[(\mathbf{r}_{12}-\mathbf{v}_{12}\tau^*)\cdot(\mathbf{v}_1-\mathbf{v}_2^*)]^2},$$

$$\sigma\hat{\sigma}_2=\mathbf{r}_{12}-\mathbf{v}_{12}\tau^*-(\mathbf{v}_1-\mathbf{v}_2^*)(\tau^{**}-\tau^*),$$

and

$$I_t(23,13)=f^{\mathrm{eq}}(123)\Theta(\mathbf{r}_{23}\cdot\mathbf{v}_{23})\Theta[\sigma^2-|\mathbf{r}_{23}|^2+(\mathbf{r}_{23}\cdot\mathbf{v}_{23})^2]\Theta[(\mathbf{v}_1-\mathbf{v}_3^*)\cdot(\mathbf{r}_{13}-\mathbf{v}_{13}\tau^*)]\Theta\Bigg(\sigma^2-[\mathbf{r}_{13}-\mathbf{v}_{13}\tau^*]^2$$

$$+\frac{1}{|\mathbf{v}_1-\mathbf{v}_3^*|^2}[(\mathbf{v}_1-\mathbf{v}_3^*)\cdot(\mathbf{r}_{13}-\mathbf{v}_{13}\tau^*)]^2\Bigg)\Theta(\tau^{**}-\tau^*)\Theta(t-\tau^{**})h[\hat{\sigma}_2\cdot(\mathbf{v}_1-\mathbf{v}_3^*)], \tag{32}$$

with

$$|\mathbf{v}_{23}|\tau^*=\mathbf{r}_{23}\cdot\mathbf{v}_{23}/|\mathbf{v}_{23}|-\sqrt{\sigma^2-|\mathbf{r}_{23}|^2+(\mathbf{r}_{23}\cdot\mathbf{v}_{23}/|\mathbf{v}_{23}|)^2}, \tag{33}$$

$$\sigma\hat{\sigma}_1=\mathbf{r}_{23}-\mathbf{v}_{23}\tau^*,$$

$$\mathbf{v}_3^*=\mathbf{v}_3+(\mathbf{v}_{23}\cdot\hat{\sigma}_1)\hat{\sigma}_1,$$

$$|\mathbf{v}_1-\mathbf{v}_3^*|^2(\tau^{**}-\tau^*)=(\mathbf{r}_{13}-\mathbf{v}_{13}\tau^*)\cdot(\mathbf{v}_1-\mathbf{v}_3^*)-\sqrt{|\mathbf{v}_1-\mathbf{v}_3^*|^2[\sigma^2-(\mathbf{r}_{13}-\mathbf{v}_{13}\tau^*)^2]+[(\mathbf{r}_{13}-\mathbf{v}_{13}\tau^*)\cdot(\mathbf{v}_1-\mathbf{v}_3^*)]^2},$$

$$\sigma\hat{\sigma}_2=\mathbf{r}_{13}-\mathbf{v}_{13}\tau^*-(\mathbf{v}_1-\mathbf{v}_3^*)(\tau^{**}-\tau^*).$$

In summary, for the precollisional phase-space region given by Eq. (14), the contributions to $f_2(12;t)$ that bring velocity correlations, f_2^c, are

$$\frac{1}{n^2}\Theta(-\mathbf{r}_{12}\cdot\mathbf{v}_{12})f_2^c(12;t)|_{|\mathbf{r}_{12}|=\sigma^+}$$

$$=qn\Theta(-\mathbf{r}_{12}\cdot\mathbf{v}_{12})\int d3\{I_t(23,12)+I_t(13,12)$$

$$+I_t(23,13)+I_t(13,23)\}|_{|\mathbf{r}_{12}|=\sigma^+}. \tag{34}$$

Then, in the precollisional region, $f_2(12;t)$ can be written as the sum of two terms

$$\Theta(-\mathbf{r}_{12}\cdot\mathbf{v}_{12})f_2(12;t)|_{|\mathbf{r}_{12}|=\sigma^+}$$

$$=\{\Theta(-\mathbf{r}_{12}\cdot\mathbf{v}_{12})\gamma n^2\varphi_0(v_1)\varphi_0(v_2)$$

$$+\Theta(-\mathbf{r}_{12}\cdot\mathbf{v}_{12})f_2^c(12;t)\}|_{|\mathbf{r}_{12}|=\sigma^+}, \tag{35}$$

where the first term includes all the contributions to f_2 that contain no velocity correlations.

We have found that velocity correlations were created at short length scales (precollisional configurations) by the dissipative dynamics of the IHS model. Starting from an equilibrium uncorrelated state, the dynamics creates these correlations by the mechanism of ring collisions, at the short time scale of the order of few mean free times.

III. EFFECT OF PRECOLLISIONAL CORRELATIONS ON OBSERVABLES

The precollisional velocity correlations modify the values of macroscopic observables. In this section the analytic expressions for collisional integrals of the form

$$\int d\hat{\sigma}\,d\mathbf{v}_1\,d\mathbf{v}_2\,\Theta(-\hat{\sigma}\cdot\mathbf{v}_{12})f_2(12;t)A(12)|_{\mathbf{r}_{12}=\sigma\hat{\sigma}} \tag{36}$$

will be studied for phase functions $A(1,2)$ that depend on the velocities of two particles and on their relative distance.

Using Eqs. (34) and (35) the collisional integral (36) can be written as

$$\int d\hat{\sigma}\,d\mathbf{v}_1\,d\mathbf{v}_2\,\Theta(-\hat{\sigma}\cdot\mathbf{v}_{12})f_2(12;t)A(12)|_{\mathbf{r}_{12}=\sigma\hat{\sigma}}$$

$$=\left(\chi-\frac{n\sigma^2 q}{\pi}R_t[1]\right)n^2\int d\hat{\sigma}\,d\mathbf{v}_1\,d\mathbf{v}_2\,\Theta(-\hat{\sigma}\cdot\mathbf{v}_{12})$$

$$\times\varphi(v_1)\varphi(v_2)A(12)|_{\mathbf{r}_{12}=\sigma\hat{\sigma}}+n^3\sigma^2 qR_t[A], \tag{37}$$

where the ring integral operator R_t is defined as

$$R_t[A]=\sigma^{-2}\int d\hat{\sigma}\,d\mathbf{v}_1\,d\mathbf{v}_2\,d3\,\Theta(-\hat{\sigma}\cdot\mathbf{v}_{12})\{I_t(23,12)$$

$$+I_t(13,12)+I_t(23,12)+I_t(13,23)\}A(12)|_{\mathbf{r}_{12}=\sigma\hat{\sigma}} \tag{38}$$

and

$$\chi = \frac{1}{n^2 \pi} \int d\hat{\sigma}\, d\mathbf{v}_1\, d\mathbf{v}_2\, \Theta(-\hat{\sigma}\cdot\mathbf{v}_{12}) f_2(12)|_{\mathbf{r}_{12}=\sigma\hat{\sigma}}, \tag{39}$$

where χ is thus the average precollisional pair correlation function at contact that should be distinguished from the postcollisional part because of the discontinuity described in the Introduction (notice that for elastic spheres, χ reduces to the pair correlation function at contact) [5].

If A is symmetric in 1 and 2, then the ring integral takes the form

$$R_t[A] = 2(R_{1t}[A] + R_{2t}[A]), \tag{40}$$

where

$$R_{1t}[A] = \sigma^{-2} \int d\hat{\sigma}\, d\mathbf{v}_1\, d\mathbf{v}_2\, d3\, \Theta(-\hat{\sigma}\cdot\mathbf{v}_{12}) \times I_t(23,12) A(12)|_{\mathbf{r}_{12}=\sigma\hat{\sigma}}, \tag{41}$$

$$R_{2t}[A] = \sigma^{-2} \int d\hat{\sigma}\, d\mathbf{v}_1\, d\mathbf{v}_2\, d3\, \Theta(-\hat{\sigma}\cdot\mathbf{v}_{12}) \times I_t(23,13) A(12)|_{\mathbf{r}_{12}=\sigma\hat{\sigma}}. \tag{42}$$

(a) Virial pressure. In granular fluids, the pressure p can only be computed with the use of the mechanical definition. In the case of the IHS model, one finds [5]

$$p = nT + \frac{\pi n^2 T \sigma^2 \chi (1-q)}{2} p_2, \tag{43}$$

where

$$p_2 = \frac{m\nu}{2\pi n \sigma^2 \chi T} \langle |\mathbf{v}_{12}\cdot\mathbf{r}_{12}| \rangle_{coll} \tag{44}$$

and ν is the collision frequency

$$\nu = \frac{1}{n} \int d\hat{\sigma}\, d\mathbf{v}_1\, d\mathbf{v}_2\, d\mathbf{r}_{12}\, f_2(12) \Theta(-\mathbf{v}_{12}\cdot\mathbf{r}_{12}) \times \delta(\mathbf{r}_{12} - \sigma\hat{\sigma}) |\mathbf{v}_{12}\cdot\mathbf{r}_{12}|. \tag{45}$$

The collisional average is defined in general by

$$\langle A \rangle_{coll} = \frac{1}{n\nu} \int d\hat{\sigma}\, d\mathbf{v}_1\, d\mathbf{v}_2\, d\mathbf{r}_{12}\, A(12) f_2(12) \Theta(-\mathbf{v}_{12}\cdot\mathbf{r}_{12}) \times \delta(\mathbf{r}_{12} - \sigma\hat{\sigma}) |\mathbf{v}_{12}\cdot\mathbf{r}_{12}|. \tag{46}$$

It can be seen that, for any one-particle probability density, the following equality holds:

$$\int d\hat{\sigma}\, d\mathbf{v}_1\, d\mathbf{v}_2\, \Theta(-\hat{\sigma}\cdot\mathbf{v}_{12}) \varphi(v_1) \varphi(v_2) m |\hat{\sigma}\cdot\mathbf{v}_{12}|^2 = 2\pi T, \tag{47}$$

where the granular temperature T is defined in two dimensions by

$$T = \frac{1}{N} \sum_i m(\mathbf{v}_i - \mathbf{v})^2, \tag{48}$$

where N is the number of particles and $\mathbf{v}$ is the hydrodynamic velocity.

With the use Eqs. (37), (46), and (47), p_2 can be expressed, to the first order in density, as

$$p_2 = 1 + \frac{n\sigma^2 q}{2\pi} \left(R_t\left[\frac{m(\hat{\sigma}\cdot\mathbf{v}_{12})^2}{T} \right] - 2R_t[1] \right), \tag{49}$$

where $\lim_{n\to 0} \chi = 1$ has been used.

The velocity correlations manifest themselves as a deviation of p_2 from one. The correction to the elastic fluid value of p_2 is proportional to q. The density dependence is more complex because in the time dependence of R_t mean free path cutoffs must me taken into account [see the discussion after Eq. (52)].

(b) Another collisional average of interest is

$$\Gamma = \left\langle \frac{\mathbf{v}_1\cdot\mathbf{v}_2}{|\mathbf{v}_1 - \mathbf{v}_2|} \right\rangle_{coll}. \tag{50}$$

In the absence of precollisional velocity correlations, Γ vanishes exactly for a fluid at rest. This property makes Γ a quantity very sensible to the presence of velocity correlations, allowing to test with accuracy theoretical predictions.

Using Eqs. (37) and (46), we obtain

$$\Gamma = \frac{1}{\nu} n^2 \sigma^3 q R_t[(\mathbf{v}_1\cdot\mathbf{v}_2)|\hat{v}_{12}\cdot\hat{\sigma}|]. \tag{51}$$

To first order in n and q, the collision frequency can be approximated as $\nu = 2n\sigma\sqrt{\pi T/m}$. Then,

$$\Gamma = \frac{qn\sigma^2}{2\sqrt{\pi T/m}} R_t[(\mathbf{v}_1\cdot\mathbf{v}_2)|\hat{v}_{12}\cdot\hat{\sigma}|]. \tag{52}$$

The ring integrals (38) depend on the time t because the distribution f_2 is time dependent. In 2D it is known that for large times, these integrals diverge with t. This problem has been extensively discussed in the theory of transport phenomena in 2D fluids (see Chap. X in [8] and references given therein). The divergence appears because one considers the dynamics of three isolated particles. The traveled distances can be, then, arbitrarily large. In a real system, the particles cannot cover large distances because of the presence of the other particles in the system. A complete resummation of ring events in the expansion (16) makes appear a cutoff of the order of the mean free path.

In the present study, the mean free path cutoff will be introduced in a phenomenological way. Consider the internal distances traveled by the particles in the ring events: l_1, l_2, and l_3 (see Fig. 1). The first way ($M1$) is to impose that

none of these three distances can exceed the mean free path ℓ. A second way $(M2)$ consists in multiplying each diagram by the exponential factor $e^{-(l_1+l_2+l_3)/\ell}$, which models the probability of collisionless motion in the homogeneous gas. Clearly, the numerical results obtained along these two ways should be looked upon as order of magnitude estimations.

We define the mean free path ring integrals R_ℓ as

$$R_\ell[A]=\sigma^{-2}\int d\hat{\sigma}\, d\mathbf{v}_1\, d\mathbf{v}_2\, d3\ \Theta(-\hat{\sigma}\cdot\mathbf{v}_{12})\{I_\ell(23,12)+I_\ell(13,12)+I_\ell(23,12)+I_\ell(13,23)\}A(12)\big|_{\mathbf{r}_{12}=\sigma\hat{\sigma}}. \tag{53}$$

Here, the integrals I_ℓ are obtained from I_t [see Eq. (29)] by replacing the step function $\Theta(t-\tau^{**})$ by the mean free path cutoff

$$\Theta(\ell-l_1)\Theta(\ell-l_2)\Theta(\ell-l_3), \tag{54}$$

for the first method $(M1)$, or by

$$\exp[-(l_1+l_2+l_3)/\ell], \tag{55}$$

for the second method $(M2)$.

According to Fig. 1 the distances l_i are given as

$$l_1=v_1\tau^{**}, \tag{56}$$

$$l_2=v_2\tau^{*}, \tag{57}$$

$$l_3=v_2^{*}(\tau^{**}-\tau^{*}) \tag{58}$$

for $I_\ell(23,12)$ and by

$$l_1=v_1\tau^{**}, \tag{59}$$

$$l_2=v_2\tau^{*}, \tag{60}$$

$$l_3=v_3^{*}(\tau^{**}-\tau^{*}) \tag{61}$$

for $I_\ell(23,13)$.

The time t has been eliminated from the ring integrals. However, it should be remembered that our expressions apply at the short time scale only [see the comment following Eq. (16)]. The mean free path integrals take into account the finite density of the system. They will yield finite values for p_2 and Γ, that can be compared with the results of MD simulations.

For a given mean free path cutoff, $R_\ell[A]$ can be evaluated numerically using Monte Carlo integrations as follows. Three-particle configurations are sampled sorting the velocities from the the Maxwellian distribution (13), the normal vector $\hat{\sigma}$ is uniformly distributed over the unit circle, and the position of the third particle is placed at random. Given a configuration, it is checked if the ring event takes place (conditions represented by step functions in Eq. (30) for $I[(23),(12)]$ or in Eq. (32) for the $I[(23),(13)]$). If the conditions are met, the integrand is evaluated and added up. A typical series of 10^9 generated configurations is enough to obtain the integrals with a precision of 1%. More efficient algorithms can be designed to speed up the calculation, but the algorithm described above is fast enough for our purposes.

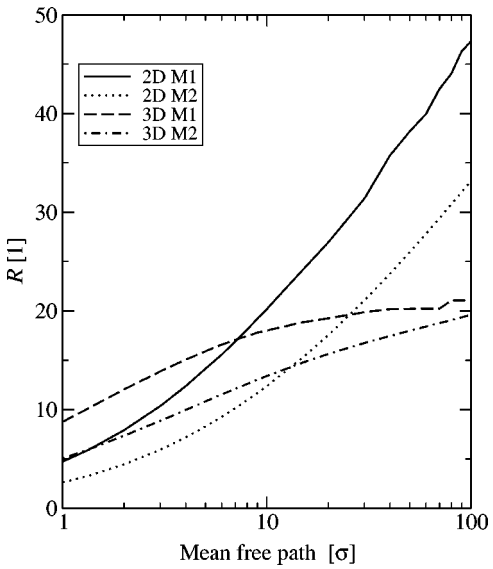

FIG. 2. Numerical evaluation of $R[1]$ as a function of the mean free path used in the cutoff (in a logarithmic scale). Data is presented for two and three dimensions using the first cutoff method $(M1)$ and the second cutoff method $(M2)$.

The analysis presented in Sec. II and in this section can be directly extended to three dimensions. Similar expressions for f_2 in the the precollisional region and for the ring integrals are obtained. However, there is a qualitative difference in the numerical computation of ring integrals. In three dimensions, these integrals are convergent for large distances, contrary to the two-dimensional case. In Fig. 2 we present the numerical evaluation of $R_\ell[1]$ as a function of the mean free path, using both cutoffs methods in two and three dimensions. It is seen that in 2D there is a logarithmic divergence with ℓ but in 3D both methods converge to the same value. Similar results are obtained for the ring integrals associated to p_2 and Γ.

IV. COMPARISON WITH MOLECULAR DYNAMICS SIMULATIONS

When a granular fluid composed of IHS particles is let to evolve freely, it cools down homogeneously. This nonsteady state can be transformed into a nonequilibrium steady state (NESS) by means of a thermostating mechanism [9,5]. After each dissipative collision, the lost energy is reinjected into the system by multiplying all the velocities by the same value, so as to keep kinetic energy constant. Due to the lack of an intrinsic energy (or time) scale in the IHS model, the multiplication of all velocities by a factor does not modify the collision sequence in the system.

In Ref. [5] molecular dynamics simulations of the NESS were done for low dissipation and moderate density. In these

TABLE I. Comparison of the values of p_2 and Γ computed in MD simulations and the theoretical predictions. Both cutoff methods are used. Results are presented at three different densities.

	Simulation	$M1$	$M2$
$n=0.05$			
Γ	$0.097q$	$0.080q$	$0.045q$
p_2	$1-0.16q$	$1-0.19q$	$1-0.11q$
$n=0.1$			
Γ	$0.27q$	$0.09q$	$0.05q$
p_2	$1-0.25q$	$1-0.25q$	$1-0.14q$
$n=0.2$			
Γ	$0.44q$	$0.09q$	$0.05q$
p_2	$1-0.65q$	$1-0.28q$	$1-0.15q$

simulations p_2 and Γ were computed showing the existence of velocity correlations. In what follows, units are chosen so that the particle masses m, diameters σ, and also the temperature T of the NESS are set to one.

In Ref. [5] the simulations were done at three different densities: $n=0.05$, $n=0.1$, and $n=0.2$, with mean free paths $\ell=6.64$, $\ell=3.10$, and $\ell=1.35$. The last value corresponds to a dense system where we do not expect to find good numerical accord with the theoretical predictions. For each density, simulations at different inelasticities were done and the results for p_2 and Γ were fitted by linear dependence of q. In Table I we present the comparison of the simulation results with theoretical predictions.

At this point, it is instructive to analyze the comparison between theory and simulations. Quite generally, the numerical comparison comes out quite well in view of the phenomenological way in which the mean free path cutoff is introduced. The agreement gets worse at higher density where the mean free path is smaller. This discrepancy is not surprising because our approach is based on a density expansion (with large mean free paths), whereas for $n=0.2$ the mean free path is of the order of the disk diameter.

Both the simulations and theory agree on the linear dependence on inelasticities and predict the same sign of the correlations. The positive sign of Γ means that the precollisional velocities of the particles are more parallel than in the elastic case. This tendency to align the velocities is a consequence of the inelastic collision law (1). After a collision with a third particle, the first pair in the ring sequence arrives to their next collision with aligned velocities. This effect is what is taken into account in the derivation presented in Sec. II.

The interpretation of the velocity correlations as reflecting the fact that particles arrive to collisions with aligned velocities is consistent with the results obtained for p_2. The contribution to the pressure from the correlations is negative, reducing the value corresponding to the elastic case: as the velocities before collision are more parallel, the transferred momentum is smaller.

In the NESS, the one-particle velocity distribution function is not Maxwellian but a distorted one. In the Boltzmann and low dissipation limit the velocity distribution function can be computed [10], obtaining

$$\varphi(v)=\varphi_T(v)[1+q\phi(v)], \tag{62}$$

where φ_T is the Maxwellian distribution,

$$\phi(v)=-\frac{m^2v^4}{8T^2}+\frac{mv^2}{T}-1, \tag{63}$$

and T is the (constant) granular temperature in the NESS. At higher densities, corrections of order n and nq are expected.

Using the same kind of arguments as in Sec. II, it can be deduced that the dissipative dynamics will give rise to velocity correlations. In this case the initial distribution function is not the thermal equilibrium one [Eq. (12)] but rather

$$\begin{aligned} f_3(123,0)&=\Theta(r_{12}-\sigma)\Theta(r_{13}-\sigma)\Theta(r_{23}-\sigma)\varphi_T(v_1)\\ &\quad\times\varphi_T(v_2)\varphi_T(v_3)\\ &\quad\times[1+q(\phi(v_1)+\phi(v_2)+\phi(v_3))]\\ &=f^{\mathrm{eq}}(123)[1+q(\phi(v_1)+\phi(v_2)+\phi(v_3))], \end{aligned} \tag{64}$$

where we have kept the first order in density and dissipation.

Using the initial condition (64), instead of the equilibrium one, in the analysis done in Sec. II we obtain that the following term that must be added to Eq. (26):

$$\begin{aligned} &qn\int d3\, f^{\mathrm{eq}}(123)e^{-t\mathcal{L}(123)}[\phi(v_1)+\phi(v_2)+\phi(v_3)]\\ &\quad=qn\int d3\, f^{\mathrm{eq}}(123)[\phi(v_1(0))+\phi(v_2(0))+\phi(v_3(0))], \end{aligned} \tag{65}$$

where we have kept only the term linear in q. The initial velocities $\mathbf{v}_i(0)$ are obtained by the elastic dynamics of three isolated particles.

Equation (65) produces velocity correlations in the precollisional region if at least one of the initial velocities $v_i(0)$ is a function of both $\mathbf{v}_1$ and $\mathbf{v}_2$, the velocities of particles 1 and 2 at time t. The previous condition can be met only if particles 1 and 2 have collided between $\tau=0$ and $\tau=t$. As we are interested in evaluating f_2 in the precollisional region (that is, particles 1 and 2 are about to collide), Eq. (65) contributes to correlations at the ring events described in Sec. II. Then, the initial velocities $v_i(0)$ are replaced by the incoming velocities v_1^{**}, v_2^{**}, and v_3^{**} (see Fig. 1). Again, we have neglected the events involving sequences of four collisions.

Then, coming from this term there are new terms J_t, similar to I_t, to be evaluated,

$$J_t(23,12)=f^{eq}(123)\Theta(\mathbf{r}_{23}\cdot\mathbf{v}_{23})\Theta(\sigma^2-|\mathbf{r}_{23}|^2+(\mathbf{r}_{23}\cdot\mathbf{v}_{23})^2)\times\Theta[(\mathbf{v}_1-\mathbf{v}_2^*)\cdot(\mathbf{r}_{12}-\mathbf{v}_{12}\tau^*)]\times\Theta\left(\sigma^2-[\mathbf{r}_{12}-\mathbf{v}_{12}\tau^*]^2+\frac{1}{|\mathbf{v}_1-\mathbf{v}_2^*|^2}\times[(\mathbf{v}_1-\mathbf{v}_2^*)\cdot(\mathbf{r}_{12}-\mathbf{v}_{12}\tau^*)]^2\right)\Theta(\tau^{**}-\tau^*)\times\Theta(t-\tau^{**})[\phi(v_1^{**})+\phi(v_2^{**})+\phi(v_3^{**})], \tag{66}$$

where the different symbols are defined in Eq. (31) and

$$\mathbf{v}_1^{**}=\mathbf{v}_1-[(\mathbf{v}_1-\mathbf{v}_2^*)\cdot\hat{\sigma}_2]\hat{\sigma}_2, \tag{67}$$

$$\mathbf{v}_2^{**}=\mathbf{v}_2+[(\mathbf{v}_1-\mathbf{v}_2^*)\cdot\hat{\sigma}_2]\hat{\sigma}_2, \tag{68}$$

$$\mathbf{v}_3^{**}=\mathbf{v}_3+(\mathbf{v}_{23}\cdot\hat{\sigma}_1)\hat{\sigma}_1. \tag{69}$$

And also

$$J_t(23,13)=f^{eq}(123)\Theta[\mathbf{r}_{23}\cdot\mathbf{v}_{23}]\Theta(\sigma^2-|\mathbf{r}_{23}|^2+(\mathbf{r}_{23}\cdot\mathbf{v}_{23})^2)\times\Theta[(\mathbf{v}_1-\mathbf{v}_3^*)\cdot(\mathbf{r}_{13}-\mathbf{v}_{13}\tau^*)]\times\Theta\left(\sigma^2-[\mathbf{r}_{13}-\mathbf{v}_{13}\tau^*]^2+\frac{1}{|\mathbf{v}_1-\mathbf{v}_3^*|^2}\times[(\mathbf{v}_1-\mathbf{v}_3^*)\cdot(\mathbf{r}_{13}-\mathbf{v}_{13}\tau^*)]^2\right)\Theta(\tau^{**}-\tau^*)\times\Theta(t-\tau^{**})[\phi(v_1^{**})+\phi(v_2^{**})+\phi(v_3^{**})], \tag{70}$$

where the different symbols are defined in Eq. (33) and

$$\mathbf{v}_1^{**}=\mathbf{v}_1-[(\mathbf{v}_1-\mathbf{v}_3^*)\cdot\hat{\sigma}_2]\hat{\sigma}_2, \tag{71}$$

$$\mathbf{v}_2^{**}=\mathbf{v}_2-(\mathbf{v}_{23}\cdot\hat{\sigma}_1)\hat{\sigma}_1, \tag{72}$$

$$\mathbf{v}_3^{**}=\mathbf{v}_3+[(\mathbf{v}_1-\mathbf{v}_3^*)\cdot\hat{\sigma}_2]\hat{\sigma}_2. \tag{73}$$

Collecting all terms, f_2^c can be written as

$$\frac{1}{n^2}\Theta(-\hat{\sigma}\cdot\mathbf{v}_{12})f_2^c(12;t)|_{\mathbf{r}_{12}=\sigma\hat{\sigma}}=qn\Theta(-\hat{\sigma}\cdot\mathbf{v}_{12})\int d3\{I_t(23,12)+I_t(13,12)+I_t(23,13)+I_t(13,23)+J_t(23,12)+J_t(13,12)+J_t(23,13)+J_t(13,23)\}|_{\mathbf{r}_{12}=\sigma\hat{\sigma}}. \tag{74}$$

The new terms in Eq. (74) represent the precollisional velocity correlations that are created by the elastic evolution of the nonequilibrium velocity distribution (62). This kind of velocity correlations have been largely studied in nonequilibrum states of elastic systems, where the velocity distributions get distorted.

TABLE II. Evaluation of Γ and p_2 using the ring integrals that include the distortion to the Maxwellian distribution. Results are presented for the same densities of Table I.

	$M1$	$M2$
$n=0.05$		
Γ	$0.085q$	$0.047q$
p_2	$1-0.19q$	$1-0.11q$
$n=0.1$		
Γ	$0.10q$	$0.05q$
p_2	$1-0.25q$	$1-0.14q$
$n=0.2$		
Γ	$0.09q$	$0.05q$
p_2	$1-0.28q$	$1-0.15q$

To compute collisional integrals, the ring integral operator must be redefined as

$$R_t[A]=\sigma^{-2}\int d\hat{\sigma}\,d\mathbf{v}_1\,d\mathbf{v}_2\,d3\,\Theta(-\hat{\sigma}\cdot\mathbf{v}_{12})\{I_t(23,12)+I_t(13,12)+I_t(23,12)+I_t(13,23)+J_t(23,12)+J_t(13,12)+J_t(23,12)+J_t(13,23)\}A(12)|_{\mathbf{r}_{12}=\sigma\hat{\sigma}}. \tag{75}$$

Mean free path cutoffs can be introduced in the same way as before. Numerical evaluation of Γ and p_2 using these ring integrals are presented in Table II. The densities are the same as in Table I. It is obtained that the distortion of the Maxwellian distribution in the NESS produces a very small contribution to velocity correlations. The most important part of the correlation is created by dynamical process described in Sec. II.

V. CONCLUSIONS

We have shown that, in the inelastic hard sphere model for granular fluids, correlated sequences of collisions give rise to precollisional velocity correlations. Inelastic collisions produce postcollisional velocity correlations even if system is initially at equilibrium. The generated correlations are propagated dynamically to the next collision. As a result, particles arrive to collision with their velocities more parallel than in elastic systems. We considered the lowest order contribution in density and inelasticity to the precollisional correlations. At this order, the correlations are produced by the so-called ring events.

In elastic systems, a small number of collisions is enough to produce local thermodynamic equilibrium, where particles have uncorrelated velocities. In the IHS model, on the contrary, a small number of collisions (two in the ring events we considered) gives rise to precollisional velocity correlations. That is, in elastic systems collisions tend to reduce velocity

correlations but, in inelastic systems, collisions create them.

Therefore, velocity correlations are always present in granular fluids. Not like in elastic fluids, where in equilibrium velocity correlations vanish. The unavoidable presence of velocity correlations in granular fluids puts into question the validity for these systems of the Boltzmann's or Enskog's kinetic theories, that neglect precollisional velocity correlations. New kinetic approaches must be developed that take into account the creation and propagation of velocity correlations in such systems.

Introducing phenomenological mean free path cutoffs, the effect of the velocity correlations in Γ (that vanishes in the absence of correlation) and the pressure is computed numerically. The numerical predictions are compared with molecular dynamics simulations results, obtaining good qualitative agreements. Both, simulations and our computations, agree that pressure must decrease due to the velocity alignment and give the correct sign of Γ, with the same order of magnitude. It would be interesting to investigate better ways to introduce the mean free path cutoff without doing a density expansion, that lead to better numerical predictions.

In a stationary state of granular systems, there is another source of precollisional velocity correlation. Correlations are produced by the distortion of the velocity distribution function in the nonequilibrium steady state. However, numerical calculations of this contribution to the correlations give a very small value.

Even though the calculations were done for the IHS model, it is expected that the mechanism studied here for the creation of velocity correlations is generic to granular systems.

It would be instructive to perform a similar analysis for time correlation functions that lead to expressions for transport coefficients in granular fluids [11].

ACKNOWLEDGMENTS

R.S acknowledges the grant from MIDEPLAN and the Grant No. 1010416 from FONDECYT. J.P. acknowledges the financial support by CNRS and the hospitality at CECAM, ENS-Lyon (France), where the major part of this research was performed.

[1] J.J. Brey, F. Moreno, and M. Ruiz-Montero, Phys. Fluids **10**, 2965 (1998).
[2] T.P.C. van Noije and M.H. Ernst, Physica A **251**, 266 (1998).
[3] T.P.C. van Noije and M.H. Ernst, Phys. Rev. E **61**, 1765 (2000).
[4] J.F. Lutsko, Phys. Rev. Lett. **77**, 2225 (1996).
[5] R. Soto and M. Mareschal, Phys. Rev. E **63**, 041303 (2001).
[6] J.J. Brey, J.W. Dufty, and A. Santos, J. Stat. Phys. **87**, 1051 (1997).
[7] T.J. Murphy and E.G.D. Cohen, in *Hard Ball Systems and the Lorentz Gas*, edited by D. Szász (Springer EMS series, Berlin, 2000), Vol. 101, pp. 29–49.
[8] P. Résibois and M. De Leener, *Classical Kinetic Theory of Fluids* (Wiley, New York, 1977).
[9] R. Soto, M. Mareschal, and M. Malek Mansour, Phys. Rev. E **62**, 3836 (2000).
[10] T.P.C. van Noije and M.H. Ernst, Granular Matter **1**, 57 (1998).
[11] I. Goldhirsch and T.P.C. van Noije, Phys. Rev. E **61**, 3241 (2000).